# 3D atlas of the pituitary gland of the model fish medaka

Muhammad Rahmad Royan[1], Khadeeja Siddique[1], Gergely Csucs[2], Maja A. Puchades[2], Rasoul Nourizadeh-Lillabadi[1], Jan G. Bjaalie[2], Christiaan V. Henkel[1], Finn-Arne Weltzien[1], Romain Fontaine[1]*

[1] Physiology unit, Faculty of Veterinary Medicine, Norwegian University of Life Sciences, Ås, Norway

[2] Institute of Basic Medical Sciences, University of Oslo, Oslo, Norway

*Corresponding author: romain.fontaine@nmbu.no

Highlights:

- We offer the first 3D atlas of a teleost pituitary, which presents a valuable resource to the endocrinology and model fish community.
- The atlas reveals the 3D spatial distribution of the seven endocrine cell types and blood vessels in the juvenile/adult male and female pituitary.
- Gene expression for *tshba* and *pomca*, as well as the population size of cells expressing these genes, displays obvious sexual dimorphism in the adult medaka pituitary.
- Multi-color *in situ* hybridization and single cell RNA-seq reveal the existence of bi-hormonal cells, co-expressing *lhb-fshb*, *fshb-tshba*, *lhb-sl*, and a few multi-hormonal cells.
- An online version of the atlas is available at https://www.nmbu.no/go/mpg-atlas.

**Abstract**

In vertebrates, the anterior pituitary plays a crucial role in regulating several essential physiological processes via the secretion of at least seven peptide hormones by different endocrine cell types. Comparative and comprehensive knowledge of the spatial distribution of those endocrine cell types is required to better understand their role during the animal life. Using medaka as the model and several combinations of multi-color fluorescence *in situ*

hybridization, we present the first 3D atlas revealing the gland-wide distribution of seven endocrine cell populations: lactotropes, thyrotropes, Lh and Fsh gonadotropes, somatotropes, and *pomca*-expressing cells (corticotropes and melanotropes) in the anterior pituitary of a teleost fish. By combining *in situ* hybridization and immunofluorescence techniques, we deciphered the location of corticotropes and melanotropes within the *pomca*-expressing cell population. The 3D localization approach reveals sexual dimorphism of *tshba*- and *pomca*-expressing cells in the adult medaka pituitary. Finally, we show the existence of bi-hormonal cells co-expressing *lhb-fshb*, *fshb-tshba* and *lhb-sl* using single-cell transcriptomics analysis and *in situ* hybridization. This study offers a solid basis for future comparative studies of the teleost pituitary and its developmental plasticity.

**Key words:** *in situ* hybridization, immunofluorescence, 3D, pituitary, medaka, hormone, atlas, single cell transcriptome, teleost

# Introduction

In vertebrates, the pituitary is considered the *chef d'orchestre* of the endocrine system, regulating several essential biological and physiological functions throughout the life cycle. Located beneath the hypothalamus, it is divided into the anterior part (adenohypophysis) and posterior part (neurohypophysis). The former comprises several endocrine cell types which produce and release specific peptide hormones (1, 2), controlling many important aspects of life, including growth, stress, metabolism, homeostasis, and reproduction (3).

During embryogenesis, different cellular developmental trajectories specify several endocrine cell types in the adenohypophysis, characterized by the hormones they produce (4). In general, the vertebrate adenohypophysis consists of lactotropes (producing prolactin; Prl), corticotropes (adrenocorticotropic hormone; Acth), thyrotropes (thyrotropin; Tsh), gonadotropes (follicle-stimulating and luteinizing hormone; Fsh and Lh), somatotropes (growth hormone; Gh), and melanotropes (melanocyte-stimulating hormone; α-Msh), which have specific roles in regulating certain physiological functions (2, 5). Teleosts, in addition, have an endocrine cell type that is unique to these animals, i.e. somatolactotropes (somatolactin; Sl) (6). In contrast to mammals and birds, Fsh and Lh are mostly secreted by distinct endocrine cell types in teleosts (7), although both transcripts or hormones have

66 sometimes been observed in the same cells in some species (8-11). Unlike mammals, teleost
67 endocrine cells are arranged in discrete zones. Lactotropes and corticotropes are commonly
68 located in the *rostral pars distalis* (RPD), thyrotropes, gonadotropes, and somatotropes in
69 the *proximal pars distalis* (PPD), and melanotropes and somatolactoropes in the *pars*
70 *intermedia* (PI) (6, 12).

71 Over the past five decades, endocrine cell type organization in the teleost pituitary has been
72 documented in various species. Despite having approximately similar patterns, the pituitary
73 endocrine cell maps exhibit differences in terms of variety of cell types that are reported.
74 For instance, the localization of endocrine cell populations in dorado fish shows only four
75 distinct types of endocrine cells across the adenohypophysis (13). By contrast, the other
76 studies describe five (Japanese medaka (14)), six (fourspine sculpin, (15); cardinal and
77 bloodfin tetra (16)), seven (greater weever fish, (17); white seabream, (18); dimerus cichlid
78 (19)), and eight (Atlantic halibut, (20); Nile tilapia, (21); saddle wrasse, (22)) cell types.

79 Even though these previous studies have provided interesting information on the spatial
80 organization of endocrine cell populations, they lack information due to the techniques
81 available and used at the time. First, the use of mid- and para-sagittal sections of the pituitary
82 to reconstruct organizational patterns of endocrine cells leads to a lack of information on the
83 lateral sides. Second, the single-labeling method and non-species specific antibodies that are
84 typically used do not provide sufficient detail on arrangements among adjacent endocrine
85 cell populations, or on the possible existence of multi-hormonal cells as described in
86 mammals (23-26). These features will be important to better understand the underlying
87 processes in fish physiology and endocrinology. Moreover, the distribution of the blood
88 vessels within the pituitary, which play an essential role by transporting the released
89 hormones, is poorly known. A better knowledge will help understand how endocrine cells
90 arranged within a vascularized system that is thought to facilitate paracrine signaling in the
91 pituitary (27). Also, since it has been shown that the pituitary is a plastic organ with changes
92 occurring at cellular and population levels (28), it is essential to describe the cell
93 composition, spatial organization, and vascularization of the pituitary in detail.

94 The Japanese medaka (*Oryzias latipes*) is a teleost model commonly used to investigate
95 vertebrate and teleost physiology, genetics, and development, due to easy access to a wide
96 range of genetic and molecular techniques (29, 30). We have recently used single-cell RNA
97 sequencing to describe seven distinct endocrine cell types (expressing *prl*, *pomca*, *fshb*, *lhb*,

98 *tshba*, *gh*, and *sl*) in the medaka pituitary (31). Here, we extend this study by describing
99 differences present in the spatial distribution of the seven endocrine cell populations, in
100 juvenile and adult fish from both sexes. Using multi-color *in situ* hybridization techniques
101 together with single-cell transcriptomics analysis, this study offers the first 3D atlas of
102 teleost pituitary endocrine cell populations, allowing the identification of differences in
103 spatial distribution patterns between sexes and stages, as well as the existence of multi-
104 hormonal cells.
105

# 106 Materials and Methods

## 107 Experimental animals

108 Juvenile (2-month old) and adult (6-month old) wild type medaka (WT, d-rR strain) were
109 reared at 28 ºC in a re-circulating water system (pH 7.5; 800 µS) with 14 hours light and 10
110 hours dark conditions. Fish were fed three times daily using artemia and artificial feed. Sex
111 determination was based on secondary sexual characteristics (32). Experiments were
112 conducted in accordance with recommendations on experimental animal welfare at the
113 Norwegian University of Life Sciences.
114

## 115 Quantitative Polymerase Chain Reaction (qPCR)

116 RNA extraction from pituitaries (n = 7) was performed as previously described in (33). Fish
117 were euthanized by immersion in ice water and pituitaries were collected and stored at -80
118 ºC in 300 µl of TRIzol® (Invitrogen, Carlsbad, USA) with 6 zirconium oxide beads (Bertin
119 Technologies, Versailles, France; diameter 1.4 µm). Later, tissues were homogenized and
120 mixed with 120 µl chloroform. The pellet was reconstituted with 14 µl of nuclease free
121 water. Due to the size of the tissue, 3 juvenile pituitaries were pooled to represent one
122 replicate of each sample. A total of 33 ng of RNA was used to synthesize cDNA using
123 SuperScript III Reverse Transcriptase (Invitrogen, Carlsbad, CA, USA) and random
124 hexamer primers (Thermofisher scientific). 5× diluted cDNA samples were analyzed in
125 duplicate, using 3 µL of the cDNA and 5 µM each of forward and reverse primer in a total
126 volume of 10 µL (**Table 1**). The parameter cycle was 10 min pre-incubation at 95 °C,
127 followed by 42 cycles of 95 °C for 10 s, 60 °C for 10 s and 72 °C for 6 s, followed by melting
128 curve analysis to assess PCR product specificity. The mRNA level was normalized using

129 *rpl7* as reference gene as it was found no significant difference of expression between
130 groups.
131

132 **Multi-color fluorescence *in situ* hybridization (Multi-color FISH)**

133 **Tissue preparation:** Fish were euthanized by immersion in ice water. Brain and pituitary
134 were taken and fixated overnight at 4 ºC in 4% paraformaldehyde (PFA, Electron
135 Microscopy Sciences, Hatfield, Pennsylvania) diluted with phosphate buffered saline with
136 Tween (PBST: PBS, 0.1%; Tween-20), approximately 50× the tissue volume. Tissue was
137 then dehydrated using a series of increasing ethanol concentrations: 25%, 50%, 75%, 96%
138 followed by a storage in 100% methanol at -20 ºC until use.

139 **Cloning and RNA probe synthesis:** DNA sequences for the probes were obtained from
140 NCBI as listed in **Table 2**. Sequences are selected according to the high expression in the
141 pituitary for those having more than one paralog in the medaka genome (*tshb* and *pomc*).
142 PCR primers for the amplification of the probe genes were designed from transcribed
143 sequences (mRNA) for each gene using Primer3 (https://primer3.ut.ee/). Following RNA
144 extraction and cDNA synthesis as described above, cDNA was used to amplify the sequence
145 of interest by PCR using Taq DNA polymerase (Thermo Fisher Scientific) with a 3-min
146 denaturation step at 94 ºC, followed by 35 cycles at 94 ºC for 15s, 50 ºC for 15s, and 72 ºC
147 for 60s, and finally 1 cycle of 72 ºC for 5 mins. The amplified PCR products were isolated
148 using a gel extraction kit (Qiagen) and cloned into the pGEM-T Easy vector (Promega)
149 following manufacturer instructions and verified by sequencing. PCR products from the
150 verified plasmids were used as template to synthetize sense and anti-sense complementary
151 RNA probes using *in vitro* transcription with T7 or SP6 RNA polymerase (Promega,
152 Madison, Wisconsin). RNA probes were tagged with dinitrophenol-11-UTP (DNP, Perkin
153 Elmer, Waltham, Massachusetts), fluorescein-12-UTP (FITC, Roche Diagnostics), or
154 digoxigenin-11-UTP (DIG, Roche Diagnostics). Finally, the probes were purified using the
155 Nucleospin RNA clean-up kit (Macherey-Nagel, Hoerdt, France) and the concentration was
156 measured using the Epoch Spectrophotometer System (BioTek, Winooski, VT, USA).

157 **Multi-color fluorescence *in situ* hybridization (FISH):** Multi-color FISH was performed
158 as previously described in (34) with minor modifications. Tissues were serially rehydrated,
159 and the pituitary was detached from the brain. Afterwards, whole pituitaries were hybridized
160 with the probes (0.11 – 3.17 ng/µl) for 18 hours at 55 ºC, and incubated with different

161 combinations of anti-DNP- (Perkin Elmer), anti-FITC-, and anti-DIG-conjugated antibodies
162 (Roche Diagnostics), followed by TAMRA- (Thermofisher), Cy5- (Perkin Elmer) and
163 FITC-conjugated tyramides (Sigma). The nuclei were stained with DAPI (1:1000, 4', 6-
164 diamidino-2-phenylindole dihydrochloride; Sigma). The absence of labeling when using
165 sense probes was used to confirm the specificity of the anti-sense probes. Whole pituitaries
166 were mounted using Vectashield H-1000 Mounting Medium (Vector, Eurobio/Abcys)
167 between microscope slides and cover slips (Menzel Glässer, VWR) with spacers
168 (Reinforcement rings, Herma) in between for the juveniles, and between two cover slips
169 with spacers for adults.

170

171 **Combined FISH and Immunofluorescence (IF)**

172 To distinguish the localization of adrenocorticotropic releasing hormone (Acth) and alpha-
173 melanocyte stimulating hormone (α-Msh) cells within *pomca*-expressing cells separately, IF
174 was performed using the antibodies shown in **Table 3**. After FISH for *pomca* labelled with
175 FITC-conjugated tyramide, the pituitaries were embedded in 3% agarose ($H_2O$) and para-
176 sagittally sectioned with 60 µm thickness using a vibratome (Leica). From a single pituitary,
177 odd and even ordered slices were processed to detect Acth and α-Msh IF, respectively.
178 Tissue slices were incubated for 10 minutes at room temperature (RT) in permeabilizing
179 buffer (0.3 % Triton in PBST) with agitation, before incubation for 1 hour at RT in blocking
180 solution (Acth: 3% normal goat serum (NGS); 0.3% Triton; 1% dimethylsulfoxide (DMSO)
181 in PBST; α-Msh: 3% NGS; 5% Triton; 7% DMSO in PBST). Sections were then incubated
182 at 4 $^{o}$C overnight with primary antibodies (diluted in blocking) or without (control), followed
183 by 4 hours at RT with secondary antibodies (diluted in blocking) with extensive PBST
184 washes in between. Nuclei were stained with DAPI (1/1000). Controls were performed as
185 described above incubating the tissue without the primary antibodies and confirming the
186 absence of fluorescent signals. The antibody dilution is provided in **Table 3**.

187

188 **Blood vessel staining**

189 Blood vessels were stained by cardiac perfusion as previously described in (35). The fish
190 were anesthetized with 0.04% Tricaine (pH 7), and the anterior abdomen was cut to let the
191 heart opening adequately wide for the injection. Afterwards, 0.05% of DiI (1,1'-Dioctadecyl-
192 3,3,3',3'-Tetramethylindocarbocyanine Perchlorate; Invitrogen) solution diluted in 4% PFA
193 (in PBS) was administered to the *bulbus arteriosus* through the ventricle using a glass

needle. The pituitary was dissected and fixated in 4% PFA (in PBS) for 2 hours in the dark before being washed 2 times with PBS and mounted as described above.

## Image processing and analysis

Fluorescent images were obtained using an LSM710 Confocal Microscope (Zeiss, Leica) with 25× (for adult pituitary) and 40× (for juvenile pituitary) objectives. Filters with wavelength of 405 (DAPI), 555 (TAMRA; Alexa-555), 633 (Cy5) and 488 (FITC; Alexa-488) nm were used. Due to the size of the adult pituitaries, the image acquisition was done from the dorsal and ventral sides of the pituitary with some overlaps in the middle. In conjunction with the microscope, ZEN software (v2009, Zeiss) was used to process the images, and ImageJ (1.52p; http://rsbweb.nih.gov/ij/) was used for processing z-projections from confocal image stacks. The dorsal and ventral stacks of adult pituitaries were aligned using HWada (https://signaling.riken.jp/en/en-tools/imagej/635/) and StackReg plugin (http://bigwww.epfl.ch/thevenaz/stackreg/), before presenting them in orthogonal views.

## 3D atlasing

While juvenile pituitaries were imaged as one block, adult pituitaries were imaged from the ventral and dorsal side with confocal imaging as described above. The two sides of the adult pituitaries were then merged using landmarks as visible with the DAPI staining. Finally, eight pituitaries labeled for different markers were aligned to the same coordinate system also using manually selected landmarks. These data were used for the creation of four 3D atlases of the pituitary gland, using the principle approaches outlined in (36).

The creation of the 3D atlases involved several steps. Merging and alignment was done using LandmarkReg (https://github.com/Tevemadar/LandmarkReg, with accompanying utilities https://github.com/Tevemadar/LandmarkReg-utils). Image stacks were saved in NIfTI format (https://imagej.nih.gov/ij/plugins/nifti.html) and converted with the "NIfTI2TopCubes" utility before the matching anatomical positions ("landmarks") were manually identified in volume-pairs. Both the signal from endocrine cells and the DAPI background were inspected, and four or more landmarks were recorded for each volume-pair. In case of ventral-dorsal half images (adult samples), a custom utility "PituBuild" was used for merging the two halves, based on partial overlap. Finally, each set of complete pituitary volumes was aligned to a common anatomical space using the "Match" utility. The resulting NIfTI volumes were then converted to TIFF stacks for viewing and analysis.

To enable 3D viewing of the pituitary atlases, data were prepared for the MeshView tool (RRID:SCR_017222, https://www.nitrc.org/projects/meshview/) developed for 3D brain atlas viewing (37). Volumes were first binarized using the "BinX" utility with a threshold value of 50. MeshGen (https://www.nitrc.org/projects/meshgen/) was then used to generate surface meshes in standard STL format (http://paulbourke.net/dataformats/stl/) before convertion using PackSTL (https://github.com/Tevemadar/MeshView-PackSTL) to allow viewing in MeshView.

## Single cell transcriptomics analysis (scRNA-seq)

We used processed scRNA-seq dataset for male and female pituitaries (31) and filtered out red blood cells to avoid noise. Next, we applied a cut-off to differentiate between cells with high and low expression for specific genes (Supp. Fig. 1). This dataset is further used to generate the pair-wise scatterplots using the R package ggplot2 (version 2_3.3.2), to show cells expressing more than one hormone-producing gene. Finally, we got 191 and 229 multiple hormone-producing cells in female and male pituitaries, respectively. We generated clustered heatmaps using pheatmap (version 1.0.12) to visualize the expression levels of hormone-producing genes in each cell expressing multiple hormones.

## Statistical analysis

Levene's test was performed to analyze the homogeneity of variance while the normality was tested using the Saphiro-Wilk Normality test. The differences in mRNA levels were evaluated using One-way ANOVA followed by Tukey *post hoc* test. The data are shown as mean + SEM (Standard Error of Mean) unless otherwise stated in the figure legend. $p < 0.05$ was used as a threshold for statistical significance.

## Data availability

All image files are available in a data repository (https://doi.org/10.18710/NOGJQ2). The 3D atlases (Fig. 1) can be found on a webpage containing explanatory videos and other types of data completing the online pituitary atlas (https://www.nmbu.no/go/mpg-atlas), allowing easy access and navigation through the data.

# Results

## 3D atlases of the medaka pituitary

Using several combinations of multi-color FISH, we combined the labeling to form four 3D pituitary atlases now available online (http://meshview.uiocloud.no/Medaka-pituitary/?JF; http://meshview.uiocloud.no/Medaka-pituitary/?JM; http://meshview.uiocloud.no/Medaka-pituitary/?AF; http://meshview.uiocloud.no/Medaka-pituitary/?AM), allowing us to precisely localize the seven endocrine cell types (*prl*, *pomca*, *tshba*, *fshb*, *lhb*, *gh* and *sl*) in the adenohypophysis of medaka.

### 1. *prl*-expressing cells (lactotropes)

In both adults and juveniles (Supp. Fig. 2), *prl*-expressing cells make up almost the entirety of the RPD from the dorsal to the ventral side of the pituitary, without any obvious difference in localization pattern between males and females. They border on and intermingle with a *pomca*-expressing cell population (Supp. Fig. 9). In some fish, a few *prl*-expressing cells are also localized peripherally in the dorsal area of PPD (data not shown).

### 2. *pomca*-expressing cells (corticotropes and melanotropes)

*pomca*-expressing cells are observed in two distinct places in the pituitary. One population is localized in the dorsal part of RPD, where it is mostly clustered in the middle if observed from transverse point of view, and the second is detected in the PI area (Supp. Fig. 3). While the first one is adjacent to and mixing with *prl*-expressing cells, in close proximity to *tshba*-expressing cells (Supp. Fig. 9), the second population intermingles with *sl*-expressing cells (Supp. Fig. 10).

### 3. *tshba*-expressing cells (thyrotropes)

*tshba*-expressing cells are localized in the dorsal side of anterior PPD towards the PN, next to the *prl*- and *pomca*-expressing cells (Supp. Fig. 4 and Supp. Fig. 9). From a transverse point of view, *tshb*-expressing cells are mostly concentrated in the middle part of the PPD (Supp. Fig. 4) where they border and mix with *fshb*-expressing cells (Supp. Fig. 11).

### 4. *fshb*-expressing cells (gonadotropes)

*fshb*-expressing cells are detected from the anterior to middle part of the PPD, distributed in both lateral sides of the pituitary from a transverse point of view (Supp. Fig. 5). These cells

291 cover the PN from a frontal point of view (Supp. Fig. 5). They border and mix with *tshba*-
292 expressing cells in the dorsal (Supp. Fig. 11), *lhb*-expressing cells in the ventral (Supp. Fig.
293 12) and *gh*-expressing cells in the posterior part of the PPD (Supp. Fig. 13).
294
295 **5. *lhb*-expressing cells (gonadotropes)**
296 In both juveniles and adults, *lhb*-expressing cells are commonly distributed in the peripheral
297 area of the PPD, covering almost the entire ventral side of the pituitary (Supp. Fig. 6). In
298 adults, *lhb*-expressing cells are also localized in the proximity of peripheral area of the PI
299 (Supp. Fig. 6). These cells border and mix with *fshb*-expressing cells in the PPD (Supp. Fig.
300 12), and with *pomca*- and *sl*-expressing cells in the PI of adult pituitary (Supp. Fig. 10).
301
302 **6. *gh*-expressing cells (somatotropes)**
303 *gh*-expressing cells are localized on the dorsal side of the PPD towards the PN area (Supp.
304 Fig. 7). Similar to *fshb*-expressing cells, which are distributed to both lateral sides of the
305 pituitary, *gh*-expressing cells are more towards the posterior part of the PPD, encompassing
306 and bordering with the PN (Supp. Fig. 7), mixing with *fshb*-expressing cells (Supp. Fig. 13).
307
308 **7. *sl*-expressing cells (somatolactotropes)**
309 *sl*-expressing cells are intermingled within *pomca*-expressing cells located in the PI (Supp.
310 Fig. 8 and Supp. Fig. 10). In the adult pituitary, these cells border and mix with *lhb*-
311 expressing cells that are detected in the proximity of the PI (Supp. Fig. 10).
312
313 **8. Distinction of Acth and α-Msh cell populations**
314 The combination of FISH for *pomca* with IF for Acth or α-Msh shows that that Acth cells
315 overlap the entire *pomca* signal, while melanotropes overlap *pomca* signals that are located
316 in the PI, both in adults (Fig. 2) and in juvenile pituitaries (Supp. Fig. 14).
317
318 **9. Blood vessels**
319 3D reconstruction shows that blood vessels encompass the entire adenohypophysis, without
320 any obvious difference observed between sexes and stages (Fig. 3).
321

322 **Sex and stage differences**

323 FISH and qPCR data did not reveal any difference in *prl*- and *gh*-expressing cell number or
324 mRNA levels between sexes and stages. In contrast, adult females show significantly higher
325 mRNA levels in both *fshb* ($p < 0.01$) and *lhb* ($p < 0.0001$) compared to the other groups,
326 while *lhb* mRNA levels are significantly higher in adult males than in juveniles ($p < 0.05$)
327 (Fig. 4), despite no obvious difference in the cell population size (Supp. Fig. 4-5). *sl* mRNA
328 levels are significantly higher in juveniles compared to adult males ($p < 0.05$) (Fig. 4)
329 without any obvious difference in cell number (Supp. Fig. 8).

330 In contrast, FISH revealed that the population of *tshba*-expressing cells is larger in adult
331 females, expanding from the anterior to the middle part of PPD, whereas in adult males and
332 juveniles they are found only in the anterior part of the PPD (Supp. Fig. 4). This agrees with
333 the significantly higher *tshba* mRNA levels observed by qPCR in the adult female group
334 compared to the other groups ($p < 0.0001$) (Fig. 4). The *tshba*-expressing cell population
335 also appears larger in juveniles than in adult males using FISH, in line with significantly
336 higher level of *tshba* mRNA observed by qPCR in juveniles compared to in adult males ($p$
337 $< 0.05$) (Fig. 4 and Supp. Fig. 4).

338 *pomca* mRNA levels in adult male are significantly higher than the other groups ($p <$
339 $0.0001$), and this agrees with the *pomca*-expressing cell population illustrated in Fig. 2,
340 Supp. Fig. 3 and Supp. Fig. 14, where there are bigger populations of *pomca* cells in adult
341 male than the other groups.

342 Despite obvious differences in mRNA transcript levels and cell number observed with qPCR
343 and FISH/IF labeling, we could not observe any difference in the proportion of each cell
344 type between males and females with the scRNA-seq data.

345

346 **Cells producing multiple hormones**

347 Using scRNA-seq data, we observed some bi-hormonal cells in the pituitary of adult medaka
348 (Fig. 5). Both sexes show a number of cells co-expressing *lhb*- and *fshb*-, *lhb*- and *tshba*-
349 and *fshb* and *tshba*. Meanwhile, some cells co-expressing *lhb* and *sl*, *fshb* and *sl*, *fshb* and
350 *prl*, *fshb* and *pomca*, *tshba* and *prl*, *tshba* and *pomca*, *prl* and *gh*, and *prl* and *pomca* are
351 unique to adult males, whereas co-expression of *fshb*- and *gh*-expressing cells is only found
352 in adult females (Fig. 5A). The co-expression between *lhb*-*fshb* and *fshb*-*tshba* in both sexes
353 and *lhb*-*sl* in adult male was confirmed using multi-color FISH (Fig. 6). While the co-

354 localization of cells expressing *lhb-fshb* and *fshb-tshba* was observed in several individuals,
355 the *lhb-sl* expressing cells were observed only in 1 out of 13 adult male pituitaries analyzed.

356 Several cells also co-express more than two hormone-encoding genes, although these are
357 rare compared with bi-hormonal cells (Fig. 5B), and in this study they could not be
358 confirmed using multi-color FISH.

359

# 360 Discussion

## 361 3D spatial distribution of endocrine cell populations and blood vessels

362 We have recently used scRNA-seq to identify and characterize seven endocrine cell types
363 in the teleost model organism medaka (31). Although a 3D atlas of the pituitary gland
364 development has been previously described in zebrafish (38), the present atlas is the first 3D
365 atlas of all pituitary endocrine cell populations in a teleost fish. It provides more precise and
366 detailed information on the distribution and organization of the different cell types, and
367 clearly demonstrate that endocrine cells are distributed differently when comparing mid-
368 sagittal with para-sagittal sections (Fig. 7).

369 As reported in coho (39) and chum salmon (40, 41), seabass (42), gilt-head seabream (43),
370 common barbel (44) and striped bass (45), we observed some lactotropes in the ventro-
371 peripheral area of the PPD. However, these cells were found only in some fish and not
372 always at the same location, which makes them difficult to map. We found Lh gonadotropes
373 in the PI, in addition to in the PPD, but only in adults, and we did not observe Lh cells in
374 RPD as reported by some studies (16, 17, 46-48). The extra-PPD localization of Lh
375 gonadotropes might be due to PPD extension (20) or Lh cell migration to other zones during
376 the ontogeny of the adenohypophysis (49). Meanwhile, several studies reported
377 somatotropes in the RPD (45, 50) and PI (51, 52), and somatolactotropes and melanotropes
378 in the PPD (13, 16-18, 51). However, we did not observe this in medaka. The wide
379 localization of Gh, Sl, and α-Msh cells in these studies might also be explained by antigenic
380 similarities as suggested in (13, 16, 53).

381 The blood vasculature is ubiquitously spread over almost the entire adenohypophysis in
382 medaka, without obvious differences between sexes and stages. This agrees with previous
383 studies in zebrafish (54, 55) showing a highly vascularized pituitary. Such complex
384 vasculature is, of course, central to the endocrinological function of the pituitary, as it allows

385 for the efficient transport of secreted hormones to peripheral organs. In addition, it may
386 facilitate intra-pituitary paracrine signaling (27).
387

388 **Sexual dimorphism of *tshba*- and *pomca*-expressing cell populations**

389 While it seems impossible to show differences of endocrine cell population between sexes
390 and stages when the data only rely on para-sagittal sections of the pituitary, whole pituitary
391 labeling methods allow their identification. For instance, we show for the first time that
392 *tshba*- and *pomca*-expressing cell populations are more numerous in adult females and
393 males, respectively. Our qPCR data on *tshba* and *pomca* levels agree with previous studies
394 in medaka (56) and further support the sexual dimorphism. In the previous medaka study,
395 androgens were suggested to be involved in *tshb* suppression in adult males via activation
396 of *tph1* transcription expressed in *pomc*-expressing cells. This is important for serotonin
397 synthesis, which plays a role in repressing the expression of some endocrine cell markers,
398 including *tshb*. We also found significantly lower *tshba* levels in adult compared to in
399 juvenile males where the androgen levels are generally lower (for review, see (57, 58)),
400 supporting the inhibitory role of androgens on *tshba* levels. It will be interesting to challenge
401 this hypothesis in future research using orchidectomy which allows for androgen clearance
402 in the medaka (59). However, although higher *tshb* levels are also observed in female half-
403 barred wrasse (60) and *tshb* levels are higher in juvenile than in adult male Atlantic salmon
404 (61), zebrafish shows no sexual dimorphism of *tshb* and *pomc* (62), suggesting species
405 differences.

406 We also observed sexual dimorphism of *fshb* and *lhb* mRNA levels in adults, in agreement
407 with a previous medaka study (56). This suggests a difference in gonadotrope cell activity
408 as we did not observe a difference in population size, also supported by the absence of
409 significant differences in Lh or Fsh cell numbers in previous studies (9, 63). In contrast, we
410 observed an increase of *lhb* mRNA levels between juvenile and adult stages, which might
411 mainly be due to an increase in cell numbers as shown in (63). Surprisingly, we did not
412 observe a significant difference in *fshb* mRNA levels between juveniles and adults, while an
413 increase in Fsh cell numbers has also been reported during sexual maturation (9). While
414 neither sexual dimorphism nor stage differences were observed in *prl* or *gh* levels, we found
415 stage difference in *sl* levels, with higher levels in juveniles than in adults. Somatolactin has
416 been associated with sexual maturation in some teleosts, such as coho salmon (64), Nile
417 tilapia (65) and flathead grey mullet (66). The upregulation of *sl* levels in teleosts is thought

418 to be related to gonadal growth, as it is highly expressed at the onset of gonadal growth and
419 lowly expressed post-ovulation (67, 68). This implies that in the current study, the adult fish
420 used might be in a post-ovulation phase while the juveniles appear to enter gonadal
421 development.
422

423 **scRNA-seq and multi-color FISH reveal the presence of multi-hormonal cells**
424 **in the adult medaka pituitary**

425 The presence of cells expressing more than one hormone in the anterior pituitary has been
426 shown in many studies, both in teleosts and in mammals (for review see (28, 69-71)). Using
427 scRNA-seq technology, multi-hormonal cells have for instance been described in the mouse
428 pituitary (72). However, using similar approaches, pituitary multi-hormonal cells have not
429 been reported in teleosts (31, 73), although some studies have documented cells producing
430 more than one hormone in the teleost pituitary (8-11).

431 Here, we show the presence of gonadotrope cells expressing both *lhb* and *fshb* which has
432 previously been reported in medaka (9) and in other teleost species (8, 10, 11). One proposed
433 underlying mechanism that could explain the existence of such bi-hormonal gonadotropes
434 is their capacity to change phenotype, with a transitory bi-hormonal state as suggested by *in*
435 *vitro* observation where Lh cells were found to become Fsh (9). We also found cells co-
436 expressing *fshb-tshba* and *sl-lhb*. Although previous immunohistochemtry studies on the
437 pituitary of several teleost species showed cross-reaction between Tsh and Lh/Fsh (43, 53)
438 and between Lh and Sl antibodies (16, 53, 74, 75), we show specific labeling of *tshb*, *fshb*,
439 *lhb*, and *sl* in the current study confirming the specificity of the probes. Therefore, the
440 observation of colocalization of *fshb-tshba* and *sl-lhb* supports that these bi-hormonal cells
441 exist in the medaka pituitary. Meanwhile, a number of studies have shown co-staining
442 between Prl, Gh and Sl (13, 20, 22, 40, 51). However, our scRNA-seq data exhibit only a
443 few cells co-expressing *prl* and *gh*. While antigenic similarities could be the reason of co-
444 staining between these cell types (13, 16, 53), their low occurrence in the medaka pituitary
445 might be the reason of being unable to observe them with FISH.

446 Within the *pomca*-expressing cell population, we observed Acth staining alone at the border
447 of the RPD/PPD and staining of both Acth and α-Msh in the PI. Co-staining between Acth
448 and α-Msh is not uncommon as Acth-immunoreactive cells have been found in RPD and PI
449 areas in other teleost species (8, 18, 20-22, 42, 43, 76). However, it must be noted that the
450 target antigen of anti-Acth used in this study and most previous studies contains the target

antigen for anti-α-Msh (https://www.uniprot.org/uniprot/P01189#PRO_0000024970). This might explain why we found both Acth and α-Msh cells in the PI. A previous study pre-incubating anti-Acth with α-Msh antigen demonstrated that Acth cells are localized in the RPD while α-Msh cells are found in the PI (21). This might also be the case in medaka.

We also show that a few cells in the adult medaka pituitary express more than two hormone-encoding genes. Despite having been reported in mammals (72), the current study is the first to show the presence of such multi-hormonal cells in the teleost pituitary. Although we could not confirm their existence using FISH, most likely because of the low number of such cells present in the pituitary, the demonstration of their existence using scRNA-seq raises questions about their origin and roles in the medaka pituitary.

Finally, the 3D atlas platform that is provided online will help research community to take a close look on the spatial distribution of endocrine cells and the vascularization of blood vessels in the pituitary.

**Author Contributions**

RF and FAW conceptualized and planned the work. RF, MAP, JB and FAW obtained funding. NR did all cloning. MRR and RF performed the experiments and acquired the imaging data. MRR and GC processed the imaging data and developed the online 3D model, supervised by MAP and JB. CH and KS analyzed the single cell transcriptome data. MRR, CH and RF wrote the paper with the inputs from all authors.

**Funding**

This study was funded by the Norwegian University of Life Sciences (to RF) and the Norwegian Research Council grants No. 251307, 255601, and 248828 (to FAW). The tools development received support from the European Union's Horizon 2020 Framework Programme for Research and Innovation under the Specific Grant Agreement No. 945539 (Human Brain Project SGA3) (to JGB) and the Research Council of Norway under Grant Agreement No. 269774 (INCF Norwegian Node) (to JGB).

**Conflict of Interest**

The authors declare that the research was conducted in the absence of any commercial or financial relationships that could be construed as a potential conflict of interest.

**Acknowledgments**

The authors thank Ms Lourdes Carreon G. Tan for her assistance in the fish husbandry.

# Figure Legends

**Figure 1.** 3D reconstruction of medaka anterior pituitary containing seven endocrine cell populations. Illustration of brain and pituitary (pointed by black arrow) of medaka from lateral view (A) and ventral view (B) (Figure is adopted and modified with permission from (63)). The navigation platform of 3D spatial distribution endocrine cell population that are now available online (C). Snapshots of 3D reconstruction of endocrine cell population from juvenile and adult medaka male and female (D). The snapshots were captured from different perspectives: free viewpoint (i), lateral (ii and iii), dorsal (iv) and ventral (iv). Four direction arrows display the direction of the pituitary (A: anterior; P: posterior; D: dorsal; V: ventral). The color legend shows the color code for each cell type.

**Figure 2.** The combination of FISH for *pomca* and IF for Acth or α-Msh allows the distinction of two clear *pomca* expressing cell populations. The distinction of Acth (green) and α-Msh (blue) producing cells from *pomca*-labelled (red) in the pituitary from adult male and female medaka. Dashed line represents the pituitary as shown in the right panel. Four direction arrows display the direction of the pituitary (A: anterior; P: posterior; D: dorsal; V: ventral).

**Figure 3.** 3D projection of blood vessels from juvenile and adult male and female medaka pituitary from the dorsal side. Left right arrow symbol shows the direction of the pituitary (A: anterior; P: posterior).

**Figure 4.** Relative mRNA levels of endocrine cell markers (*prl*, *tshba*, *fshb*, *lhb*, *gh*, *sl* and *pomca*) in juvenile and adult medaka males and females (juvenile male, JM; juvenile female, JF; adult male, AM; adult female, AF). Graphs are provided as mean + SEM, and jitter dots

509 represent N. Different letters display statistical differences ($p < 0.05$) between groups as
510 evaluated by One-way ANOVA followed by Tukey *post hoc* test.

511 **Figure 5.** scRNA-seq data reveal the presence of bi-hormonal and multi-hormonal cells in
512 the medaka pituitary. Pair wise plots of 2228 cells in female and 3245 cells in male pituitary
513 (A). Colored by filtered cells (gray), *lhb* expressing cells (green), *fshb* expressing cells
514 (darkolivegreen), *tshba* expressing cells (cyan), *sl* expressing cells (red), *prl* expressing cells
515 (blue), *gh* expressing cells (magenta), *pomca* expressing cells (darkgrey) and cells
516 expressing more than one endocrine gene (purple). Light grey cells represent the cells where
517 gene expression for the investigated hormone is considered as part of the background. Axes
518 are log normalized. Heatmap of seven hormone-encoding genes of the female and male
519 pituitary (B). Each row represents one cell, and left side indicates cell clustering. Low
520 expressions are shown in blue and high expressions are shown in red. Color bars on the
521 left indicates how different cell types clustered on the basis of expression in each cell. Black
522 arrows show cells that strongly express more than two hormone-encoding genes.

523 **Figure 6.** Multi-color FISH reveals some cells co-expressing more than one hormone-
524 encoding genes in the medaka pituitary. Confocal plane confirming colocalization of *lhb*
525 and *fshb* labelings (A), and *fshb* and *tshb* (B) labelings in both male and female adult medaka
526 pituitary. Confocal plane showing the colocalization of *lhb* and *sl* in adult male (C). White
527 arrows show cells whose mRNAs are co-expressed, while yellow arrows show cells that do
528 not (can be used as control of probe´s specificity). The location of the bi-hormonal cells is
529 in the proximity of red rectangle as illustrated in the schematic drawing of pituitary in left
530 panels.

531 **Figure 7.** Schematic illustration showing differences in distribution of endocrine cell
532 population between mid-sagittal and para-sagittal section of the medaka pituitary. The
533 schemas are drawn based on mid- (A) and para-sagittal (B) point of view. C) Transverse
534 view of medaka pituitary showing approximate location of mid-sagittal (red) and para-
535 sagittal sections (green). Four direction arrows display the direction of the pituitary (A:
536 anterior; P: posterior; D: dorsal; V: ventral).

537 **Supp. Fig. 1.** Density plots of hormone-encoding genes in the pituitary of adult male (A)
538 and female (B) medaka. Red line represents a cut-off to differentiate between the cells with
539 high gene expression (considered as endocrine cells) and low gene expression (considered
540 as background and non-endocrine cells).

541 **Supp. Fig. 2-8.** Orthogonal view of each endocrine cell types in juvenile and adult male and
542 female medaka. (2, *prl*; 3, *pomca*; 4, *tshba*; 5, *fshb*; 6, *lhb*; 7, *gh*; 8, *sl*). The pictures were
543 captured from different perspectives: transverse (i), frontal (ii) and para-sagittal (iii). Up
544 down arrow symbol shows the direction of the pituitary (A: anterior; P: posterior; D: dorsal;
545 V: ventral).

546 **Supp. Fig. 9-13.** Transverse views of multi-color FISH of endocrine cells in juvenile and
547 adult male and female medaka. (9, *prl-tshba-pomca*; 10, *sl-lhb-pomca*; 11, *fshb-tshba*; 12,
548 *fshb-lhb*; 13, *fshb-gh*) (A: anterior; P: posterior; D: dorsal; V: ventral).

549 **Supp. Fig. 14.** The combination of FISH for *pomca* and IF for Acth or α-Msh allows the
550 distinction of two clear *pomca* expressing cell populations. The distinction of Acth (green)
551 and α-Msh (blue) producing cells from *pomca*-labelled (red) in the pituitary from juvenile
552 male and female medaka. Dashed line represents the pituitary as shown in the right panel.
553 Four direction arrows display the direction of the pituitary (A: anterior; P: posterior; D:
554 dorsal; V: ventral).

555 **Table 1.** Primer sequences used for the mRNA level analysis in the medaka pituitary.

556 **Table 2.** Primer sequences used to make the *in situ* hybridization (ISH) probes of seven
557 endocrine cell types in the medaka pituitary.

558 **Table 3.** Primary and secondary antibodies used for immunofluorescence (IF) to distinguish
559 Acth and α-Msh cells from *pomca*-expressing cells in the medaka pituitary.

560

561 # References


562 1. Yeung C-M, Chan C-B, Leung P-S, Cheng CHK. Cells of the anterior pituitary. The
563 International Journal of Biochemistry & Cell Biology. 2006;38(9):1441-9.
564 2. Ooi GT, Tawadros N, Escalona RM. Pituitary cell lines and their endocrine applications.
565 Molecular and Cellular Endocrinology. 2004;228(1):1-21.
566 3. Melmed S. The pituitary: Academic press; 2010.
567 4. Brinkmeier ML, Davis SW, Carninci P, MacDonald JW, Kawai J, Ghosh D, et al. Discovery of
568 transcriptional regulators and signaling pathways in the developing pituitary gland by
569 bioinformatic and genomic approaches. Genomics. 2009;93(5):449-60.
570 5. Le Tissier PR, Hodson DJ, Lafont C, Fontanaud P, Schaeffer M, Mollard P. Anterior pituitary
571 cell networks. Frontiers in Neuroendocrinology. 2012;33(3):252-66.
572 6. Kaneko T. Cell Biology of Somatolactin. In: Jeon KW, editor. International Review of
573 Cytology. 169: Academic Press; 1996. p. 1-24.

7. Weltzien F-A, Hildahl J, Hodne K, Okubo K, Haug TM. Embryonic development of gonadotrope cells and gonadotropic hormones – Lessons from model fish. Molecular and Cellular Endocrinology. 2014;385(1):18-27.
8. Hernández MPGa, García Ayala A, Zandbergen MA, Agulleiro B. Investigation into the duality of gonadotropic cells of Mediterranean yellowtail (Seriola dumerilii, Risso 1810): immunocytochemical and ultrastructural studies. General and Comparative Endocrinology. 2002;128(1):25-35.
9. Fontaine R, Ager-Wick E, Hodne K, Weltzien F-A. Plasticity in medaka gonadotropes via cell proliferation and phenotypic conversion. Journal of Endocrinology. 2020;245(1):21.
10. Candelma M, Fontaine R, Colella S, Santojanni A, Weltzien F-A, Carnevali O. Gonadotropin characterization, localization and expression in the European hake (Merluccius merluccius). Reproduction. 2017;153(2):123.
11. Golan M, Biran J, Levavi-Sivan B. A Novel Model for Development, Organization, and Function of Gonadotropes in Fish Pituitary. Frontiers in Endocrinology. 2014;5(182).
12. Schreibman MP, Leatherland JF, McKeown BA. Functional Morphology of the Teleost Pituitary Gland. American Zoologist. 2015;13(3):719-42.
13. Honji RM, Nóbrega RH, Pandolfi M, Shimizu A, Borella MI, Moreira RG. Immunohistochemical study of pituitary cells in wild and captive Salminus hilarii (Characiformes: Characidae) females during the annual reproductive cycle. SpringerPlus. 2013;2(1):460.
14. Aoki K, Umeura H. Cell Types in the Pituitary of the Medaka (Oryzias latipes). Endocrinologia Japonica. 1970;17(1):45-55.
15. Mukai T, Oota Y. Histological Changes in the Pituitary, Thyroid Gland and Gonads of the Fourspine Sculpin (Cottus kazika) during Downstream Migration. Zoological Science. 1995;12(1):91-7.
16. Camacho LR, Pozzi AG, de Freitas EG, Shimizu A, Pandolfi M. Morphological and immunohistochemical comparison of the pituitary gland between a tropical Paracheirodon axelrodi and a subtropical Aphyocharax anisitsi characids (Characiformes: Characidae) %J Neotropical Ichthyology. 2020;18.
17. Sánchez Cala F, Portillo A, Martín del Río MP, Mancera JM. Immunocytochemical characterization of adenohypophyseal cells in the greater weever fish (Trachinus draco). Tissue and Cell. 2003;35(3):169-78.
18. Segura-Noguera MM, Laíz-Carrión R, Martín del Río MP, Mancera JM. An Immunocytochemical Study of the Pituitary Gland of the White Seabream (Diplodus Sargus). The Histochemical Journal. 2000;32(12):733-42.
19. Pandolfi M, Cánepa MM, Meijide FJ, Alonso F, Vázquez GR, Maggese MC, et al. Studies on the reproductive and developmental biology of Cichlasoma dimerus (Percifomes, Cichlidae). Biocell. 2009;33(1):1-18.
20. Weltzien F-A, Norberg B, Helvik JV, Andersen Ø, Swanson P, Andersson E. Identification and localization of eight distinct hormone-producing cell types in the pituitary of male Atlantic halibut (Hippoglossus hippoglossus L.). Comparative Biochemistry and Physiology Part A: Molecular & Integrative Physiology. 2003;134(2):315-27.
21. Kasper RS, Shved N, Takahashi A, Reinecke M, Eppler E. A systematic immunohistochemical survey of the distribution patterns of GH, prolactin, somatolactin, β–TSH, β–FSH, β–LH, ACTH, and α–MSH in the adenohypophysis of Oreochromis niloticus, the Nile tilapia. Cell and Tissue Research. 2006;325(2):303-13.
22. Parhar IS, Nagahama Y, Grau EG, Ross RM. Immunocytochemical and Ultrastructural Identification of Pituitary Cell Types in the Protogynous Thalassoma duperrey during Adult Sexual Ontogeny. 1998;15 %J Zoological Science(2):263-76, 14.
23. Childs GV. Development of gonadotropes may involve cyclic transdifferentiation of growth hormone cells. Archives of physiology and biochemistry. 2002;110(1-2):42-9.

24. Childs GV. Multipotential pituitary cells that contain adrenocorticotropin (ACTH) and other pituitary hormones. Trends in Endocrinology & Metabolism. 1991;2(3):112-7.
25. Frawley LS, Boockfor FR. Mammosomatotropes: Presence and Functions in Normal and Neoplastic Pituitary Tissue. Endocrine Reviews. 1991;12(4):337-55.
26. Fukami K, Tasaka K, Mizuki J, Kasahara K, Masumoto N, Miyake A, et al. Bihormonal Cells Secreting Both Prolactin and Gonadotropins in Normal Rat Pituitary Cells. Endocrine Journal. 1997;44(6):819-26.
27. Ben-Shlomo A, Melmed S. Chapter 2 - Hypothalamic Regulation of Anterior Pituitary Function. In: Melmed S, editor. The Pituitary (Third Edition). San Diego: Academic Press; 2011. p. 21-45.
28. Fontaine R, Ciani E, Haug TM, Hodne K, Ager-Wick E, Baker DM, et al. Gonadotrope plasticity at cellular, population and structural levels: A comparison between fishes and mammals. General and Comparative Endocrinology. 2020;287:113344.
29. Wittbrodt J, Shima A, Schartl M. Medaka — a model organism from the far east. Nature Reviews Genetics. 2002;3(1):53-64.
30. Naruse K. Genetics, Genomics, and Biological Resources in the Medaka, Oryzias latipes. In: Naruse K, Tanaka M, Takeda H, editors. Medaka: A Model for Organogenesis, Human Disease, and Evolution. Tokyo: Springer Japan; 2011. p. 19-37.
31. Siddique K, Ager-Wick E, Fontaine R, Weltzien F-A, Henkel CV. Characterization of hormone-producing cell types in the medaka pituitary gland using single-cell RNA-seq. bioRxiv. 2020.
32. Kenji Murata, Masato Kinoshita, Kiyoshi Naruse, Minoru Tanaka, Kamei Y. Looking at Adult Medaka. In: Kenji Murata, Masato Kinoshita, Kiyoshi Naruse, Minoru Tanaka, Kamei Y, editors. Medaka: Biology, Management, and Experimental Protocols. 2: John Wiley & Sons; 2019. p. 49-95.
33. Burow S, Fontaine R, von Krogh K, Mayer I, Nourizadeh-Lillabadi R, Hollander-Cohen L, et al. Medaka follicle-stimulating hormone (Fsh) and luteinizing hormone (Lh): Developmental profiles of pituitary protein and gene expression levels. General and Comparative Endocrinology. 2019;272:93-108.
34. Fontaine R, Affaticati P, Yamamoto K, Jolly C, Bureau C, Baloche S, et al. Dopamine Inhibits Reproduction in Female Zebrafish (Danio rerio) via Three Pituitary D2 Receptor Subtypes. Endocrinology. 2013;154(2):807-18.
35. Fontaine R, Weltzien F-A. Labeling of Blood Vessels in the Teleost Brain and Pituitary Using Cardiac Perfusion with a DiI-fixative. Journal of Visualized Experiments. 2019(148):e59768.
36. Bjerke IE, Øvsthus M, Papp EA, Yates SC, Silvestri L, Fiorilli J, et al. Data integration through brain atlasing: Human Brain Project tools and strategies. European Psychiatry. 2018;50:70-6.
37. Yates SC, Groeneboom NE, Coello C, Lichtenthaler SF, Kuhn P-H, Demuth H-U, et al. QUINT: Workflow for Quantification and Spatial Analysis of Features in Histological Images From Rodent Brain. Frontiers in Neuroinformatics. 2019;13(75).
38. Chapman SC, Sawitzke AL, Campbell DS, Schoenwolf GC. A three-dimensional atlas of pituitary gland development in the zebrafish. Journal of Comparative Neurology. 2005;487(4):428-40.
39. Farbridge KJ, McDonald-Jones G, McLean CL, Lowry PJ, Etches RJ, Leatherland JF. The development of monoclonal antibodies against salmon (Oncorhynchus kisutch and O. keta) pituitary hormones and their immunohistochemical identification. General and Comparative Endocrinology. 1990;79(3):361-74.
40. Naito N, Takahashi A, Nakai Y, Kawauchi H, Hirano T. Immunocytochemical identification of the prolactin-secreting cells in the teleost pituitary with an antiserum to chum salmon prolactin. General and Comparative Endocrinology. 1983;50(2):282-91.

41. Wagner GF, McKeown BA. The immunocytochemical localization of pituitary somatotrops in the genus Oncorhynchus using an antiserum to growth hormone of chum salmon (Oncorhynchus keta). Cell Tissue Res. 1983;231(3):693-7.
42. Cambré ML, Verdonck W, Ollevier F, Vandesande F, Batten TFC, Kühn ER. Immunocytochemical identification and localization of the different cell types in the pituitary of the seabass (Dicentrarchus labrax). General and Comparative Endocrinology. 1986;61(3):368-75.
43. Quesada J, Lozano MT, Ortega A, Agulleiro B. Immunocytochemical and ultrastructural characterization of the cell types in the adenohypophysis of Sparus aurata L. (Teleost). General and Comparative Endocrinology. 1988;72(2):209-25.
44. Toubeau G, Poilve A, Baras E, Nonclercq D, De Moor S, Beckers JF, et al. Immunocytochemical study of cell type distribution in the pituitary of Barbus barbus (Teleostei, Cyprinidae). General and Comparative Endocrinology. 1991;83(1):35-47.
45. Huang L, Specker JL. Growth Hormone- and Prolactin-Producing Cells in the Pituitary Gland of Striped Bass (Morone saxatilis): Immunocytochemical Characterization at Different Life Stages. General and Comparative Endocrinology. 1994;94(2):225-36.
46. Borella MI, Venturieri R, Mancera JM. Immunocytochemical identification of adenohypophyseal cells in the pirarucu (Arapaima gigas), an Amazonian basal teleost. Fish Physiology and Biochemistry. 2009;35(1):3-16.
47. Olivereau M, Nagahama Y. Immunocytochemistry of gonadotropic cells in the pituitary of some teleost species. General and Comparative Endocrinology. 1983;50(2):252-60.
48. Dubourg P, Burzawa-Gerard E, Chambolle P, Kah O. Light and electron microscopic identification of gonadotrophic cells in the pituitary gland of the goldfish by means of immunocytochemistry. General and Comparative Endocrinology. 1985;59(3):472-81.
49. Nozaki M, Naito N, Swanson P, Miyata K, Nakai Y, Oota Y, et al. Salmonid pituitary gonadotrophs I. Distinct cellular distributions of two gonadotropins, GTH I and GTH II. General and Comparative Endocrinology. 1990;77(3):348-57.
50. Grandi G, Colombo G, Chicca M. Immunocytochemical studies on the pituitary gland of Anguilla anguilla L., in relation to early growth stages and diet-induced sex differentiation. General and Comparative Endocrinology. 2003;131(1):66-76.
51. García-Hernández MP, García-Ayala A, Elbal MT, Agulleiro B. The adenohypophysis of Mediterranean yellowtail, Seriola dumerilii (Risso, 1810): an immunocytochemical study. Tissue and Cell. 1996;28(5):577-85.
52. Grandi G, Chicca M. Early development of the pituitary gland in Acipenser naccarii (Chondrostei, Acipenseriformes): an immunocytochemical study. Anatomy and Embryology. 2004;208(4):311-21.
53. Batten TFC. Immunocytochemical demonstration of pituitary cell types in the teleost Poecilia latipinna, by light and electron microscopy. General and Comparative Endocrinology. 1986;63(1):139-54.
54. Gutnick A, Blechman J, Kaslin J, Herwig L, Belting H-G, Affolter M, et al. The Hypothalamic Neuropeptide Oxytocin Is Required for Formation of the Neurovascular Interface of the Pituitary. Developmental Cell. 2011;21(4):642-54.
55. Golan M, Zelinger E, Zohar Y, Levavi-Sivan B. Architecture of GnRH-Gonadotrope-Vasculature Reveals a Dual Mode of Gonadotropin Regulation in Fish. Endocrinology. 2015;156(11):4163-73.
56. Kawabata-Sakata Y, Nishiike Y, Fleming T, Kikuchi Y, Okubo K. Androgen-dependent sexual dimorphism in pituitary tryptophan hydroxylase expression: relevance to sex differences in pituitary hormones. Proceedings of the Royal Society B: Biological Sciences. 2020;287(1928):20200713.
57. Taranger GL, Carrillo M, Schulz RW, Fontaine P, Zanuy S, Felip A, et al. Control of puberty in farmed fish. General and Comparative Endocrinology. 2010;165(3):483-515.

724 58. Borg B. Androgens in teleost fishes. Comparative Biochemistry and Physiology Part C:
725 Pharmacology, Toxicology and Endocrinology. 1994;109(3):219-45.
726 59. Royan MR, Kanda S, Kayo D, Song W, Ge W, Weltzien F-A, et al. Gonadectomy and Blood
727 Sampling Procedures in the Small Size Teleost Model Japanese Medaka (Oryzias latipes). JoVE.
728 2020(166):e62006.
729 60. Ohta K, Mine T, Yamaguchi A, Matsuyama M. Sexually dimorphic expression of pituitary
730 glycoprotein hormones in a sex-changing fish (Pseudolabrus sieboldi). Journal of Experimental
731 Zoology Part A: Ecological Genetics and Physiology. 2008;309A(9):534-41.
732 61. Martin SAM, Wallner W, Youngson AF, Smith T. Differential expression of Atlantic salmon
733 thyrotropin β subunit mRNA and its cDNA sequence. Journal of Fish Biology. 1999;54(4):757-66.
734 62. He W, Dai X, Chen X, He J, Yin Z. Zebrafish pituitary gene expression before and after
735 sexual maturation. Journal of Endocrinology. 2014;221(3):429.
736 63. Fontaine R, Ager-Wick E, Hodne K, Weltzien F-A. Plasticity of Lh cells caused by cell
737 proliferation and recruitment of existing cells. Journal of Endocrinology. 2019;240(2):361.
738 64. Rand-Weaver M, Swanson P, Kawauchi H, Dickhoff WW. Somatolactin, a novel pituitary
739 protein: purification and plasma levels during reproductive maturation of coho salmon. Journal of
740 Endocrinology. 1992;133(3):393.
741 65. Mousa MA, Mousa SA. Immunocytochemical Study on the Localization and Distribution of
742 the Somatolactin Cells in the Pituitary Gland and the Brain ofOreochromis niloticus(Teleostei,
743 Cichlidae). General and Comparative Endocrinology. 1999;113(2):197-211.
744 66. Mousa MA, Mousa SA. Implication of somatolactin in the regulation of sexual maturation
745 and spawning of Mugil cephalus. Journal of Experimental Zoology. 2000;287(1):62-73.
746 67. Benedet S, Björnsson BT, Taranger GL, Andersson E. Cloning of somatolactin alpha, beta
747 forms and the somatolactin receptor in Atlantic salmon: seasonal expression profile in pituitary
748 and ovary of maturing female broodstock. Reproductive biology and endocrinology. 2008;6:42-.
749 68. Onuma T, Kitahashi T, Taniyama S, Saito D, Ando H, Urano A. Changes in expression of
750 genes encoding gonadotropin subunits and growth hormone/prolactin/somatolactin family
751 hormones during final maturation and freshwater adaptation in prespawning chum salmon.
752 Endocrine. 2003;20(1):23-33.
753 69. Fontaine R, Royan MR, von Krogh K, Weltzien F-A, Baker DM. Direct and Indirect Effects of
754 Sex Steroids on Gonadotrope Cell Plasticity in the Teleost Fish Pituitary. Frontiers in
755 Endocrinology. 2020;11(858).
756 70. Childs GV, MacNicol AM, MacNicol MC. Molecular Mechanisms of Pituitary Cell Plasticity.
757 Frontiers in Endocrinology. 2020;11(656).
758 71. Rizzoti K. Adult pituitary progenitors/stem cells: from in vitro characterization to in vivo
759 function. 2010;32(12):2053-62.
760 72. Ho Y, Hu P, Peel MT, Chen S, Camara PG, Epstein DJ, et al. Single-cell transcriptomic
761 analysis of adult mouse pituitary reveals sexual dimorphism and physiologic demand-induced
762 cellular plasticity. Protein & Cell. 2020;11(8):565-83.
763 73. Fabian P, Tseng KC, Smeeton J, Lancman JJ, Dong PDS, Cerny R, et al. Lineage analysis
764 reveals an endodermal contribution to the vertebrate pituitary. Science. 2020;370(6515):463-7.
765 74. Batten T, Ball JN, Benjamin M. Ultrastructure of the adenohypophysis in the teleost
766 Poecilia latipinna. Cell and Tissue Research. 1975;161(2):239-61.
767 75. Margolis-Kazan H, Peute J, Schreibman MP, Halpern LR. Ultrastructural localization of
768 gonadotropin and luteinizing hormone releasing hormone in the pituitary gland of a teleost fish
769 (the platyfish). Journal of Experimental Zoology. 1981;215(1):99-102.
770 76. Yan HY, Thomas P. Histochemical and immunocytochemical identification of the pituitary
771 cell types in three sciaenid fishes: Atlantic croaker (Micropogonias undulatus), spotted seatrout
772 (Cynoscion nebulosus), and red drum (Sciaenops ocellatus). General and Comparative
773 Endocrinology. 1991;84(3):389-400.

774

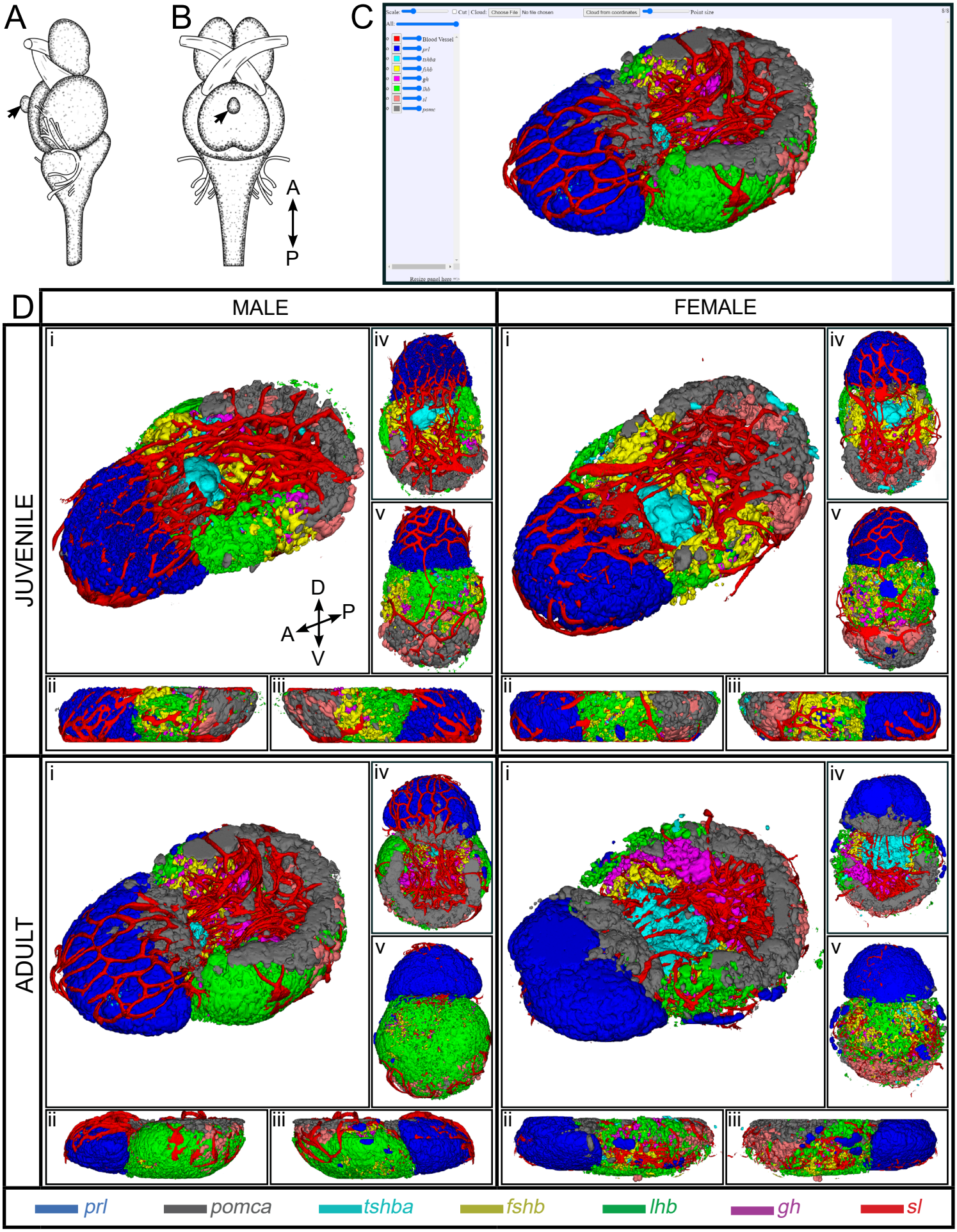
A
B
A
P
C
Blood Vessel
prl
tshba
fshb
lhb
gh
sl
pomc
D
MALE
FEMALE
JUVENILE
ADULT
i
ii
iii
iv
v
D
P
A
V
prl
pomca
tshba
fshb
lhb
gh
sl

FIGURE 1

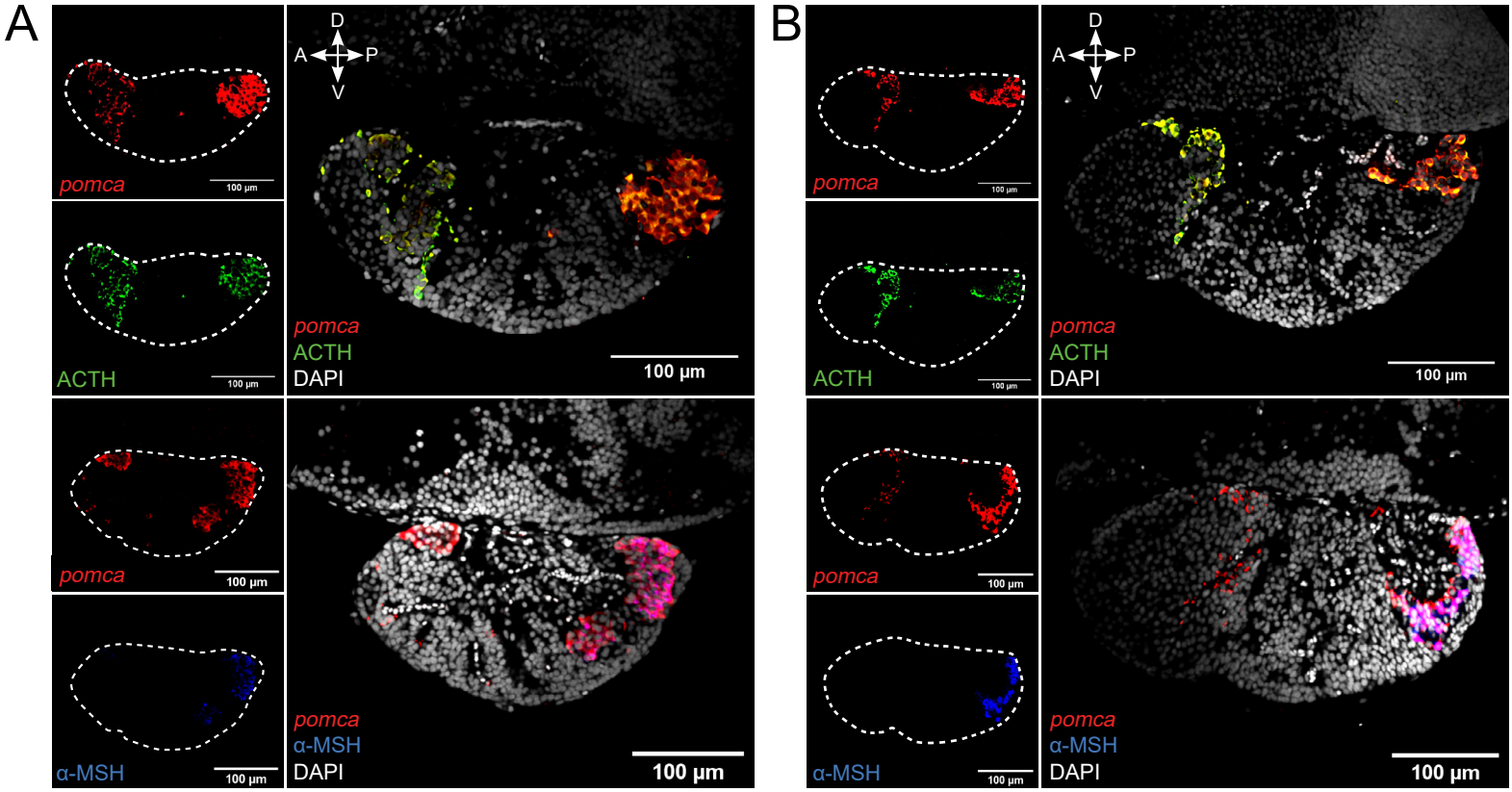


FIGURE 2

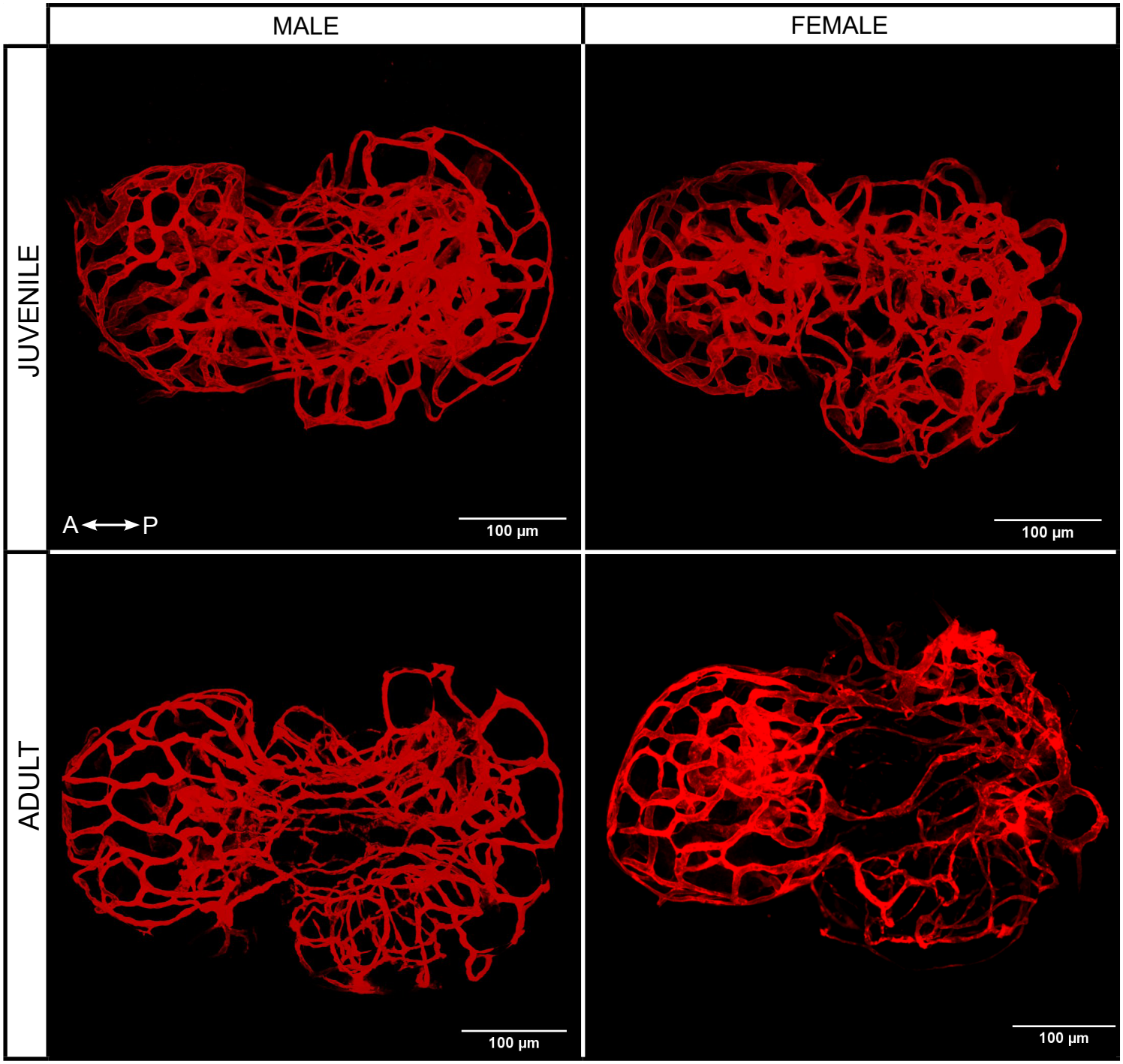


FIGURE 3

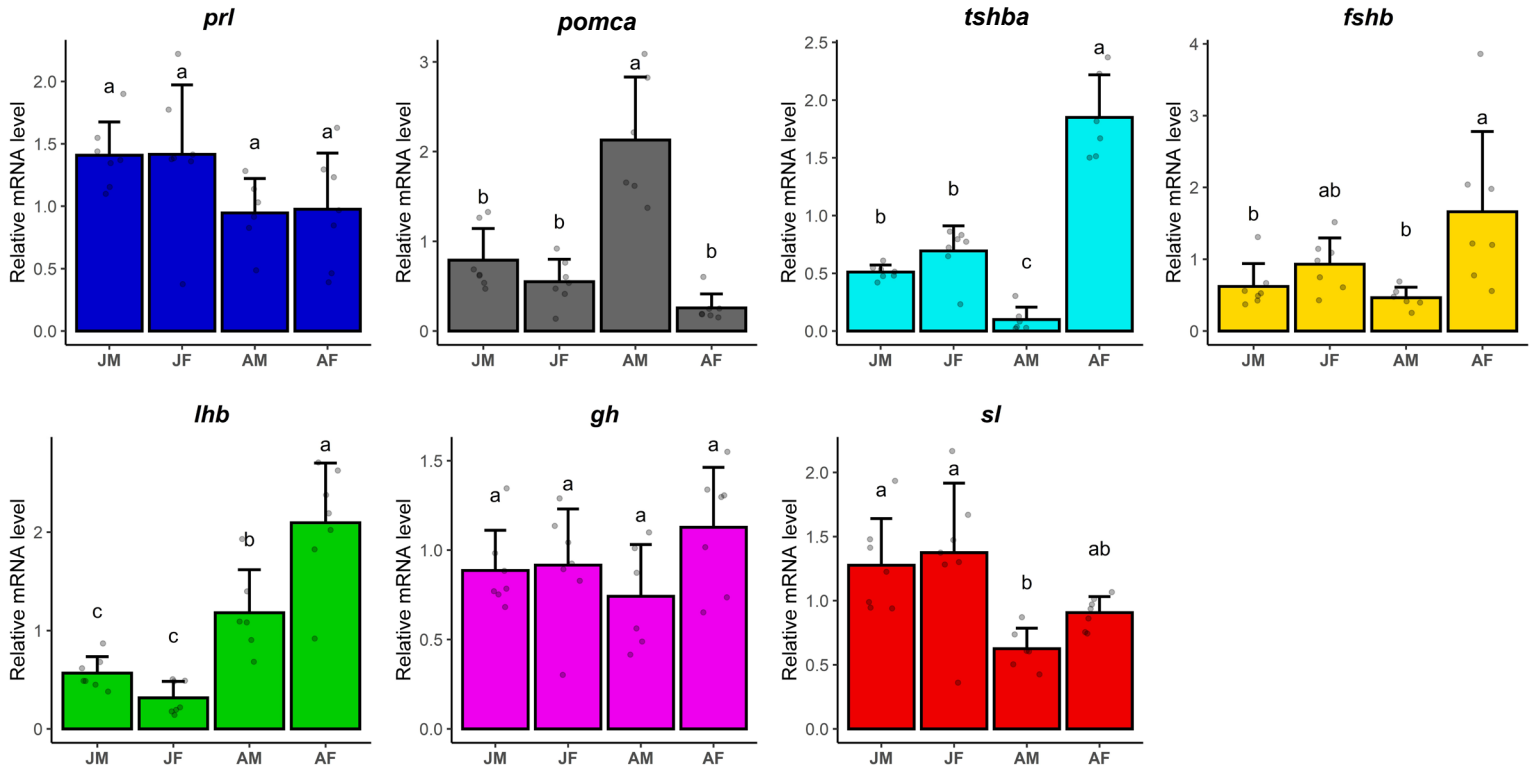


FIGURE 4

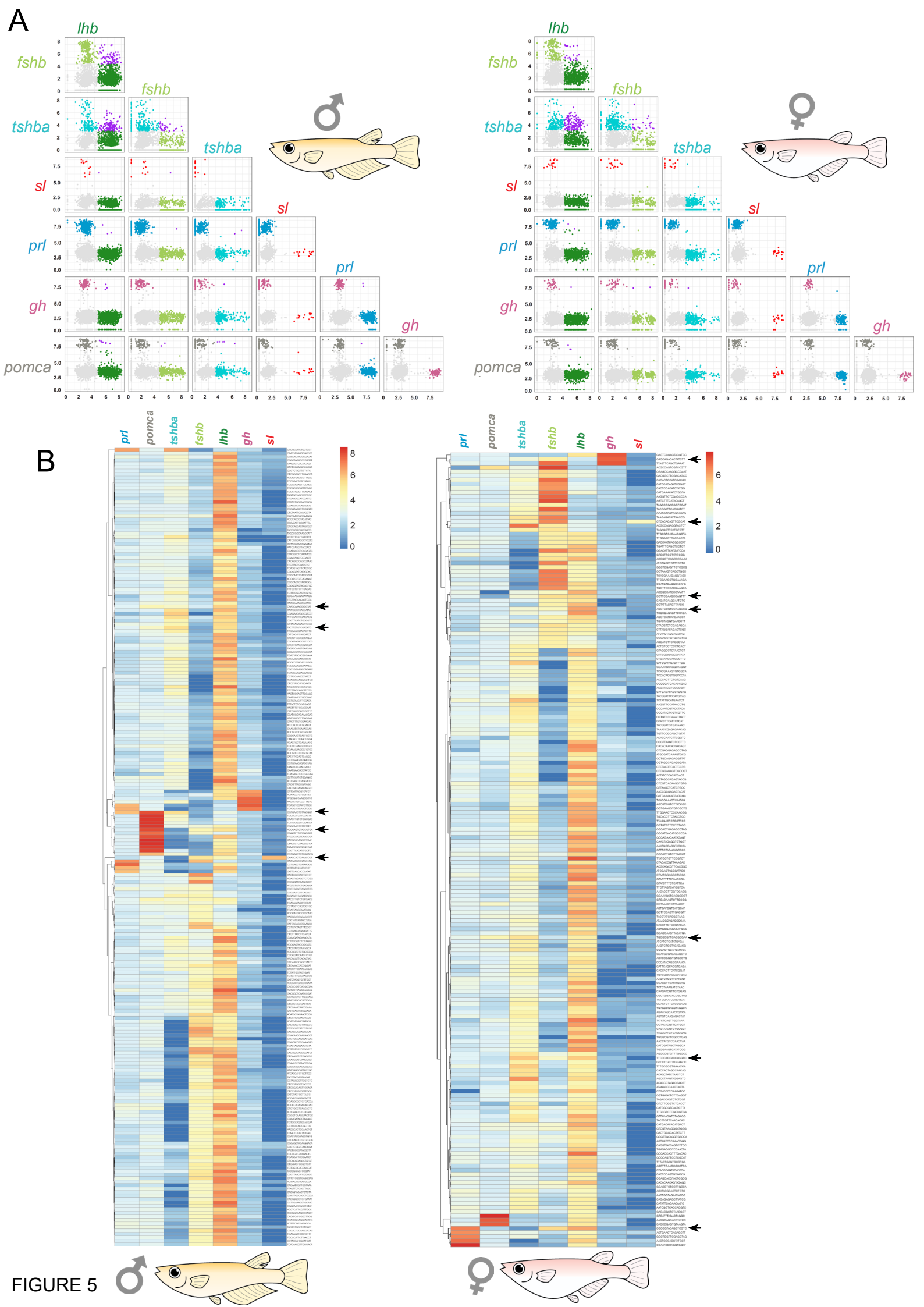
A
lhb
fshb
tshba
sl
prl
gh
pomca
♂
♀
B
prl
pomca
tshba
fshb
lhb
gh
sl

FIGURE 5

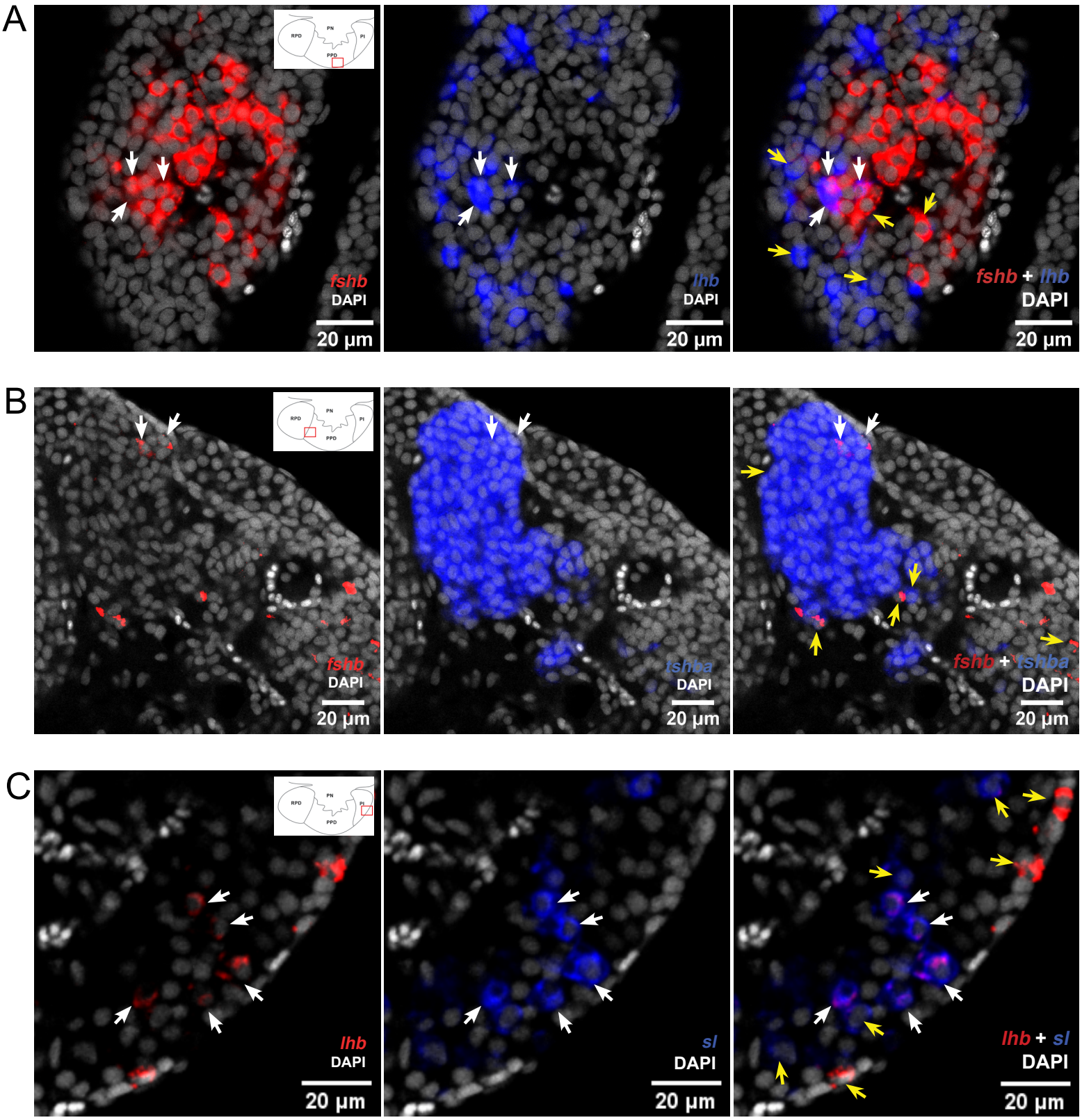
A
RPD
PN
PI
PPD
fshb
DAPI
20 µm
lhb
DAPI
20 µm
fshb + lhb
DAPI
20 µm
B
RPD
PN
PI
PPD
fshb
DAPI
20 µm
tshba
DAPI
20 µm
fshb + tshba
DAPI
20 µm
C
RPD
PN
PI
PPD
lhb
DAPI
20 µm
sl
DAPI
20 µm
lhb + sl
DAPI
20 µm

FIGURE 6

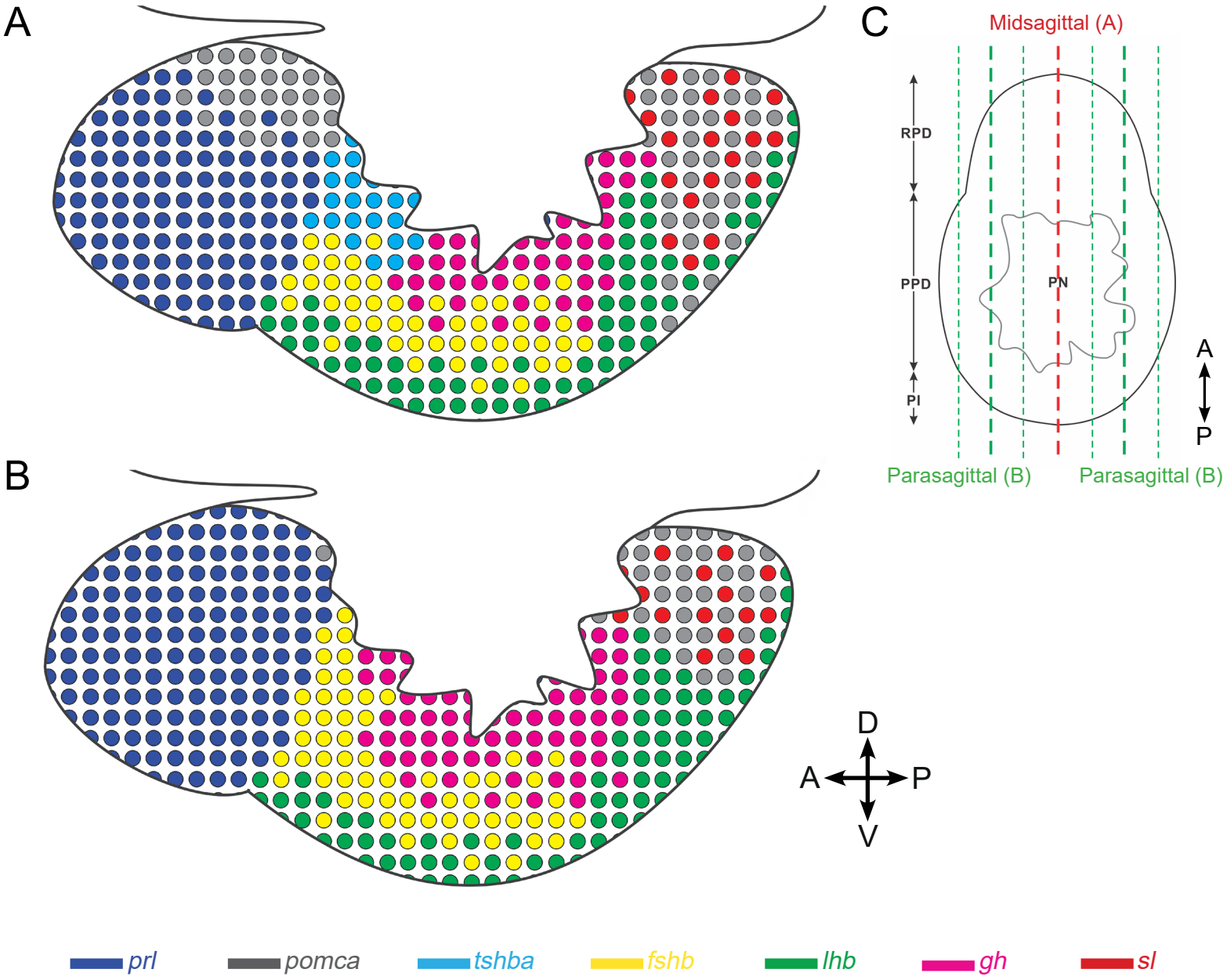
A
B
C
Midsagittal (A)
RPD
PPD
PI
PN
A
P
Parasagittal (B)
Parasagittal (B)
D
A
P
V
prl
pomca
tshba
fshb
lhb
gh
sl

FIGURE 7

| Gene Name | Sequence (5' - 3') | Ensembl Gene Name | Accession Number (NCBI/Ensembl) | Amplicon size (bp) | Efficiency | Reference |
|---|---|---|---|---|---|---|
| *rpl7* | F: TGCTTTGGTGGAGAAAGCTC | *rpl7* | NM_001104870 | 98 | 2.03 | (Burow et al., 2019) |
| | R: TGGCAGGCTTGAAGTTCTTT | | ENSORLG00000007967 | | | |
| *prl* | F: TCAGATGGGAACCAGAGGAC | *prl1* | XM_004071867.4 | 85 | 1.987 | This study |
| | R: GATGTCCACGGCTTTACACA | | ENSORLG00000016928 | | | |
| *tshba* | F: ATGTGGAGAAGCCAGAATGC | *tshba* | XM_004068796.4 | 88 | 2 | This study |
| | R: CTCATGTTGCTGTCCCTTGA | | ENSORLG00000029251 | | | |
| *lhb* | F: CCACTGCCTTACCAAGGACC | *lhb* | NM_001137653.2 | 100 | 2 | (Hildahl et al., 2012) |
| | R: AGGAAGCTCAAATGTCTTGTAG | | ENSORLG00000003553 | | | |
| *fshb* | F: GACGGTGCTACCATGAGGAT | *fshb* | NM_001309017.1 | 73 | 2.03 | (Burow et al., 2019) |
| | R: TCCCCACTGCAGATCTTTTC | | ENSORLG00000029237 | | | |
| *gh* | F: TCGCTCTTTGTCTGGGAGTT | *gh1* | XM_004084500.3 | 102 | 1.94 | This study |
| | R: ACATTCTGATTGGCCCTGAT | | ENSORLG00000019556 | | | |
| *pomca* | F: GTGGTGGTTGTCGGTGGG | *pomca* | XM_004066456.3 | 122 | 1.956 | This study |
| | R: GTGAGGTCAGAGCGGCAG | | ENSORLG00000025908 | | | |
| *sl* | F: CACCAAAGCATTACCCATCC | *smtla* | NM_001104790.1 | 87 | 1.965 | This study |
| | R: ACCAGCATCAGCACAGAATG | | ENSORLG00000013460 | | | |

TABLE 1

| Gene | Sequence (5' - 3') | Ensmbl gene name | Accession Number (NCBI/Ensembl) | PCR product size (bp) | Reference |
|---|---|---|---|---|---|
| *lhb* | F: CACAGCCTGCAGATACATGAG | *lhb* | NM_001137653.2 | 318 | Hildahl et al. (2012) |
| | R: AGGAAGCTCAAATGTCTTGTAG | | ENSORLG00000003553 | | |
| *fshb* | F: GAGGAAGCAACACTTTCAGC | *fshb* | NM_001309017.1 | 500 | Hodne et al (2019) |
| | R: GCACAGTTTCTTTATTTCAGTGC | | ENSORLG00000029237 | | |
| *pomca* | F: ATGTATACCGTTTGGTTGCT | *pomca* | XM_004066456.3 | 515 | This study |
| | R: AAATGCTTCATCTTGTAGGAG | | ENSORLG00000025908 | | |
| *sl* | F: CCCATCTTTTCACTGTAAGT | *smtla* | NM_001104790.1 | 506 | This study |
| | R: ATACTGGAAGGCACCTTGTT | | ENSORLG00000013460 | | |
| *prl* | F: GAAAGACCGAGGAGGAACTG | *prl1* | XM_004071867.4 | 381 | This study |
| | R: TTGCAGAGTTGGACAGGACC | | ENSORLG00000016928 | | |
| *gh* | F: TCTCTGCAGACTGAGGAACA | *gh1* | XM_004084500.3 | 501 | This study |
| | R: AGCCACAGTCAGGTAGGTCT | | ENSORLG00000019556 | | |
| *tshba* | F: ACAGGCTAAACTCAAGTTAA | *tshba* | XM_004068796.4 | 473 | This study |
| | R: AGGATCATATAGGTGCTCTG | | ENSORLG00000029251 | | |

TABLE 2

| Antibody | Dilution | Source | Reference |
|---|---|---|---|
| Rabbit anti-human ACTH antibody | 1:1000 | abcam (ab74976) | (Romanò et al., 2017) |
| Rabbit anti-human α-MSH antibody | 1:3000 | abcam (ab123811) | (Pravdivyi et al., 2015) |
| Goat anti-rabbit antibody (Alexa-555) | 1:500 | Invitrogen (A21429) | (Hodne et al., 2019) |

TABLE 3